Physica A 650 (2024) 129995

Contents lists available at ScienceDirect

Physica A

journal homepage: www.elsevier.com/locate/physa

Effective interactions in protein solutions with and without clustering

Fajun Zhang [a,*], Michal K. Feustel [a], Maximilian W.A. Skoda [b], Robert M.J. Jacobs [c], Felix Roosen-Runge [d], Tilo Seydel [e], Michael Sztucki [f], Frank Schreiber [a]

[a] Universität Tübingen, Institut für Angewandte Physik, Auf der Morgenstelle 10, Tübingen, 72076, Germany
[b] ISIS Facility, STFC, Rutherford Appleton Laboratory, Didcot, OX11 0QX, United Kindom
[c] Department for Chemistry, University of Oxford, Oxford, OX1 3TA, United Kindom
[d] Malmö University, Department of Biomedical Science, Malmö, 205 06, Sweden
[e] Institut Max von Laue - Paul Langevin (ILL), 71 avenue des Martyrs, Gernoble, 38000, France
[f] The European Synchrotron Radiation Facility (ESRF), 71 avenue des Martyrs, Gernoble, 38000, France

ARTICLE INFO

MSC:
00-01
99-00

Keywords:
Protein interaction
Protein clustering
Competing interactions
SAXS
BSA
BLG
Lysozyme

ABSTRACT

Protein interactions in solution and the question of cluster formation are of paramount importance to a wide range of research fields and industrial applications. Protein clustering can arise due to a delicate interplay between the short-range attraction and the long-range repulsion in the interaction potential. This study employs small angle X-ray scattering (SAXS) to examine the clustering behavior of three protein systems in solution: bovine serum albumin (BSA), bovine β-lactoglobulin (BLG) and lysozyme (LYZ) under varying protein concentrations, ionic strengths and temperatures. The goal is to elucidate the influence of the attractive potential's nature on clustering behavior. BSA serves as a reference system, where electrostatic repulsions dominate the effective interactions, resulting in a mean protein–protein distance as a function of protein concentration which follows the 1/3 power law and precludes protein cluster formation. In contrast, BLG and LYZ solutions exhibit exponents less than 1/3, indicating concentration-dependent cluster formation. The effective interactions are well described using a two-Yukawa type potential comprising a long-ranged repulsion and a short-ranged attraction. While increasing ionic strength by adding NaCl reduced repulsion and correlation in all three systems, the response of protein solutions to ionic strength differed for clustering systems of BLG and LYZ. BLG solutions exhibited a reduced attraction with increasing ionic strength, leading to cluster dissolution, while LYZ solutions experienced enhanced attraction, favoring larger cluster formation. Notably, BLG solutions showed minimal temperature dependence, while LYZ solutions exhibited increased attraction with decreasing temperature, further promoting cluster formation. These results demonstrate the crucial role of short-ranged attractions of specific nature in determining protein clustering behavior. A thorough understanding of protein interactions is essential for predicting protein clustering and phase behavior.

1. Introduction

The intricate phase behavior of biological systems is crucial to our understanding of, *inter alia*, protein crystallization [1–6], protein condensation related diseases [1,2,6–10], as well as the phase behavior of cytoplasm within cells [11–14]. These phenomena,

* Corresponding author.
E-mail address: fajun.zhang@uni-tuebingen.de (F. Zhang).

https://doi.org/10.1016/j.physa.2024.129995

Available online 25 July 2024

from the perspective of soft matter physics, are analogous to phase transitions, which are governed by the effective interactions between macromolecules in solution [1,2,6,10,15,16]. Protein interactions in aqueous solutions are typically complex and influenced by various environmental parameters including concentration, ionic strength, salt type, pH, and temperature [4–10,16–28].

Globular proteins with net charges are frequently modeled as a system of small charged colloids [8,10,16]. The effective interactions between proteins can be quantitatively determined using small angle X-ray scattering (SAXS) [10,29]. Scattering intensity distributions from a charged particle solution, such as charged colloids, proteins, DNA, or polyelectrolytes, often exhibit a pronounced peak at a finite q value. This indicates the existence of time-averaged ordered structure in these systems. The underlying principle of this phenomenon is primarily attributed to the electrostatic repulsion between charged particles, which is aptly described by the DLVO theory, encompassing Coulombic repulsion and van der Waals attraction.

A simple geometry argument leads to the dependence of the average inter-particle distance, d, on the concentration, c, in a charged colloidal solution (or protein solutions) follows a relation of $d \propto c^{-1/3}$. This ordering phenomenon has been extensively studied in various protein systems, revealing a wide range of exponent values. For example, BSA [30–33], apoferritin [34,35], ovalbumin [36] and Cytochrome C at high pH [37] typically exhibit exponents close to 1/3. In contrast, lysozyme displays a significantly weaker dependence with an exponent far below 1/3. [9] This observation prompted a series of investigations into dynamic protein clustering [9,24,38–44]. The reduced exponents in these cases are attributed to the formation of protein clusters as concentration increases. Further studies have revealed that the formation of protein clusters arises from the interplay of long-range repulsion and short-range attraction forces [45–50]. Theoretical models and simulations suggest that in such systems, the structure factor exhibits a peak due to intermediate-range ordering, which plays a dominant role in the scattering intensity maximum [43,51]. Therefore, the concentration-dependent shift of the peak position may not be a definitive indicator of protein clustering [43].

Protein clusters formed under the influence of competing interaction potentials exhibit a short lifetime, rendering them highly dynamic and transient in nature. [40,42,43] It is crucial to distinguish these dynamic clusters from mesoscopic protein clusters, which can serve as precursors for protein crystallization [9,25,40–44,52,53]. These dynamic clusters are small, typically about 10 nm or smaller. [42,44] Their lifetime is normally much shorter than the one of mesoscopic clusters. [40,42] Dynamic clusters constitute a substantial portion of the total protein in solution, significantly impacting the scattering correlation peak. [9,41,44] In contrast, mesoscopic clusters occupy a very small volume fraction and only contribute primarily to the increase of scattering intensity in the low q region in small angle scattering profiles. These clusters can also be partially removed through filtration. [41] Due to their short lifetime and loose structure, dynamic clusters are not considered viable precursors for crystal nucleation. [54]

Extensive studies on various proteins have unveiled the hallmarks of protein clustering, including the characteristically weak concentration dependence of the correlation peak in SAXS/SANS profiles [9,38,40,43,44]. These observations suggest that the effective interactions between proteins can be effectively described by a two-Yukawa type potential, encompassing both short-range attraction and long-range repulsion. Additionally, dynamic studies have demonstrated that protein clusters may exhibit limited lifetimes, determined by the delicate balance between these opposing potentials [40,42,43,55]. The origin of the long-range repulsion is typically attributed to electrostatic interactions arising from protein surface charges. However, the source or nature of the attraction potential remains unclear in many cases, even for well-established systems like lysozyme. We propose that the precise origin of attraction may vary from protein to protein, leading to diverse clustering behaviors.

In this study, we conducted SAXS experiments on three distinct protein solutions, varying concentration, ionic strength, and temperatures. Employing appropriate models, we fitted the SAXS data to obtain quantitative insights into the interaction potentials governing these protein systems. Our primary objective was to compare the clustering behavior exhibited by these protein systems and elucidate the impact of the attraction potential's nature on clustering behavior.

2. Experimental

2.1. Materials and sample preparation

Bovine serum albumin (BSA) (product No. A7906), bovine β-lactoglobulin (BLG) (product No. L3908 with a 90% purity) and salt (NaCl) were purchased from Sigma-Aldrich. BSA was lyophilized powder, essentially globulin free, essentially protease free, ≥98% (agarose gel electrophoresis) Hen egg white Lysozyme was purchased from Fluka (L7651, three times crystallized, dialyzed, and lyophilized).

All samples were prepared by mixing the required amount of salt stock solution, deionized (18.2 MΩ) degassed Millipore water and protein stock solution. Stock solutions were prepared by dissolving the protein powder or salt in deionized degassed Millipore water. The concentration of proteins in solutions was determined by UV absorption measurements using the extinction coefficients of 0.96, 0.667 and 2.64 L g^{-1} cm^{-1} at a wavelength of 278 nm for BLG, BSA and LYZ, respectively [56]. A Seven Easy pH instrument from Mettler Toledo was used to monitor the pH of the solutions.

2.2. Small angle X-ray scattering (SAXS) and data analysis

SAXS measurements were performed at the ESRF, Grenoble, France, at beamline ID02. The samples were measured using a flow-through capillary cell with a diameter of 1.0 mm and a thickness of about 10 μm at sample-to-detector distances of 1 and 5 m for BLG and 2 m for BSA and LYZ. The sample in the scattering volume was exchanged for every exposure. For each sample, 10 exposures of 0.1 s or 20 exposures of 0.05 s each were measured. The 2D intensity pattern was corrected to an absolute scale and azimuthally averaged to obtain the intensity profiles. Afterwards, the solvent background was subtracted. More detailed information

on data reduction and q-resolution calibration can be found in the literature [36,57,58]. Additional SAXS data were collected at station 6.2 of the Synchrotron Radiation Source (SRS) at the Daresbury Laboratory, Warrington, U.K., details can be found in our previous publication [59].

Small-angle X-ray scattering data can be used to obtain information on the pair interaction potential [60–62]. The scattering intensity, $I(q)$, for a non-spherical system, can be expressed by

$$I(q) = N(\Delta\rho)^2 V^2 P(q)\bar{S}(q). \tag{1}$$

where $q = \frac{4\pi}{\lambda}\sin(\theta/2)$ is the scattering vector, θ is the scattering angle, λ is the X-ray wavelength, N is the number of protein molecules per unit volume in the solution, $\Delta\rho = \rho_p - \rho_s$ is the electron density difference between the solvent and the solute, and V is the volume of a single protein. $P(q)$ is the form factor of a given protein, i.e. the scattering from a single protein molecule after orientation averaging. A form factor of an oblate ellipsoid with semi-axes a and b is used to model the proteins. The structure factor $\bar{S}(q)$ is calculated using the average structure factor approximation from a monodisperse spherical system [63], with an effective sphere diameter which is calculated from a virtual sphere with the same second virial coefficient as the ellipsoid [64,65]. In the following parts, for simplicity, we use $S(q)$ to denote $\bar{S}(q)$. To describe the effective interactions in protein solution, structure factors derived from model potentials were used for data analysis. Data fitting for the determination of the interaction potential was preformed on IGOR Pro with macros developed at NIST [66]. More details of data analysis could be found in previous work [36,59].

3. Results and discussion

3.1. Concentration dependent protein clustering and interactions

3.1.1. Concentration dependent ordering and cluster formation

BSA has been used as a model system for understanding the interactions using small angle scattering techniques [30,31,59,67]. BSA has a molecular weight of 66.7 kDa, 583 amino acids and an isoelectric point (pI) of 4.6 [28,59]. SAXS profiles for BSA solutions without added salt are shown in Fig. 1a. In agreement with the literature, a pronounced correlation peak is visible from the lowest concentration (10 mg/ml), the peak position shifts to higher q values with increasing concentration. The peak intensity, however, first increases and decreases after reaching a maximum around 200 mg/ml. This is because of the strong decay of intensity from the form factor, i.e. the scattering of individual proteins.

SAXS data for protein BLG solutions with various concentrations are shown in Fig. 1b. Without added salt, BLG solutions have a constant pH of 6.8. A BLG monomer consists of 162 amino acids and has a molecular mass of about 18.3 kDa. Under physiological conditions, it is found predominantly as a dimer [68]. With a pI of 5.2, it is acidic and carries a net charge of −10 e at neutral pH [69]. The negative net charge of BLG dimers dominates the interactions between proteins in solution. Across a wide range of protein concentrations, from 14 to 200 mg/ml, SAXS profiles consistently reveal a prominent correlation peak, indicative of electrostatic repulsion between BLG molecules. However, the peak positions, representing the average inter-protein distance in solution, exhibit a very weak concentration dependence, increasing slightly with increasing protein concentration. This observation is consistent with our previous work. [44] By employing a combination of SAXS, neutron spin echo (NSE) and neutron back scattering (NBS), we confirm that BLG in solutions form compact clusters that are static on the observation time scale of several nanoseconds. [44]

SAXS data for protein LYZ solutions with various concentrations are shown in Fig. 1c. LYZ has a molecular weight of 14.3 kDa, 129 amino acids and a pI of 10.8. The clustering effect in LYZ solutions has been well-documented [7,9,38,40,41,43,70,71]. The peak position in SAXS/SANS profiles is very sensitive to protein concentration, ionic strength, pH and temperature. For instance, a systematic study by Stradner et al. [38] revealed that for LYZ solutions at pH 7.8 in HEPES buffer, the cluster–cluster peaks remain nearly constant in the concentration range from 169 to 317 mg/ml. In a broader range of protein concentration, as demonstrated in the study by Shukla et al. [41], the peak position does shift towards higher q values with increasing concentration, but this shift is much slower than the 1/3 power law as discussed further below.

During LYZ sample preparation, no buffer was employed, causing the dissolution of proteins to release protons into the solution. Consequently, the pH of the solution decreases with increasing protein concentration. Above 20 mg/mL, the pH stabilizes around 4.6. Since the pI of LYZ is about 10.8, the decreasing pH intensifies the surface charge, leading to a stronger repulsion. The SAXS results in Fig. 1c clearly demonstrate a shift of the peak position towards higher q with increasing protein concentration.

As discussed in the introduction, under typical colloid conditions, when charged particles are well dispersed in solution, the average inter-particle distance follows a power law of $d \propto c^{-1/3}$. In the current cases, SAXS data for both BSA and LYZ display a clear shift of the correlation peak with increasing concentration, whereas for BLG the shift is rather weak. We determine the inter-particle distance directly from the peak position and plot it as a function of protein concentration in Fig. 2. In all cases, a good linear relationship is observed on a logarithmic scale. The exponents are obtained from the slope, which are 0.34, 0.12 and 0.24 for BSA, BLG and LYZ, respectively.

The position of the peak in the SAXS pattern represents the average inter-protein distance, and its concentration-dependent variation provides insights into the ordering behavior of the protein solution. The results of the plots reveal striking differences between the three protein systems. For BSA, the exponent is 0.34 nearly 1/3, in good agreement with the ordering effect of charged particles in solution. It is worth noting that for higher protein concentration above 200 mg/ml, the exponent increases to 0.4, as reported previously. [33] This deviation from the 1/3 power law is likely attributed to the ellipsoidal shape of BSA and its deformation at high packing densities. In contrast, for BLG, the exponent is only 0.12, suggesting the presence of additional attractive interactions that could promote cluster formation. For LYZ, which is known to form clusters even in unbuffered solutions, the exponent is 0.24, indicating a weak clustering. The pH is responsible for this, as described earlier, the pH of LYZ solutions decreases from around 7 to 4.6 upon dissolution. This decrease in pH leads to a higher surface charge of the proteins as the pI is larger than 7. As a result, the strength of repulsion is enhanced, which partially weakens the cluster formation.

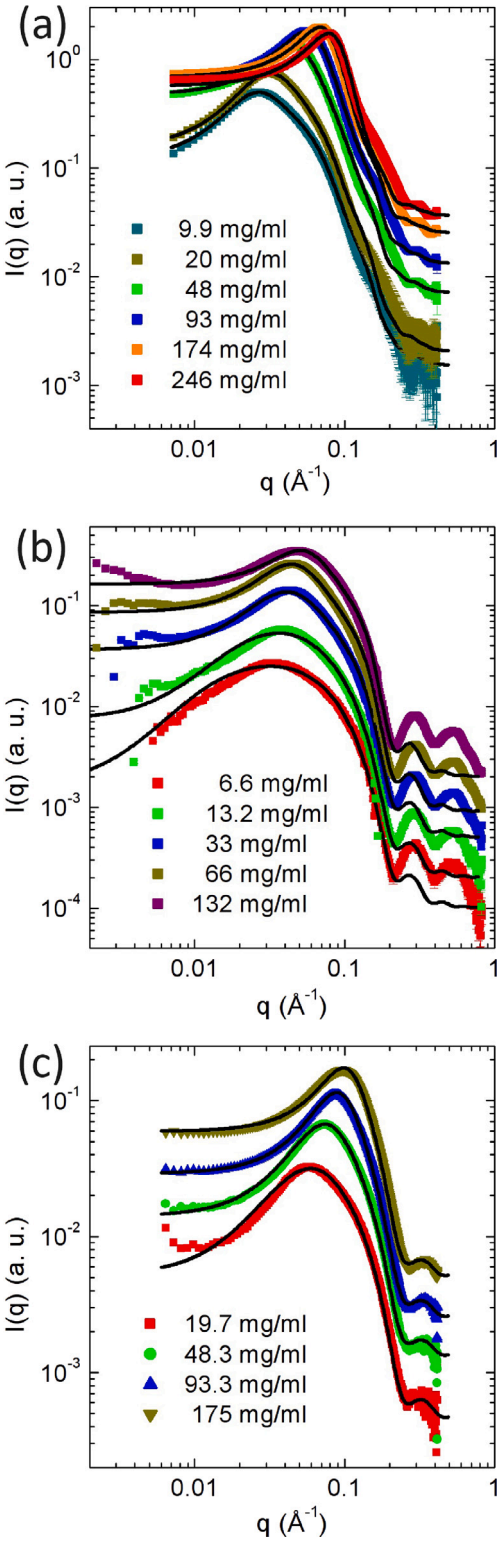

Fig. 1. SAXS profiles for three protein systems at different concentrations and the corresponding structure factor from model fitting: (**a**) BSA. (**b**) BLG and (**c**) LYZ. The solid black lines are the corresponding data fits.

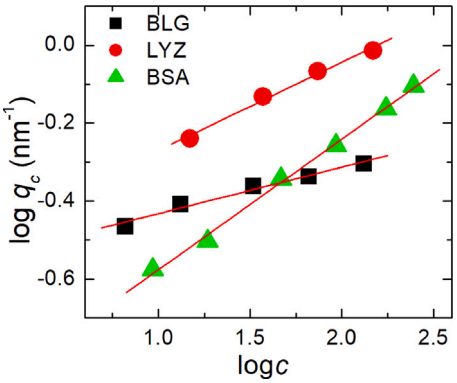

Fig. 2. Plot of peak position as a function of protein concentration in log scale. The slope gives the exponent of concentration dependent.

3.1.2. *Effective protein–protein interactions characterized by SAXS*

The effective interactions between proteins can be quantitatively determined from SAXS measurements. The interaction potential is closely related to the structure factor contribution in SAXS. For globular proteins carrying net charges and interact mainly via a screened Coulomb (SC) potential, the corresponding structure factor has been calculated by Hayter, Penfold and Hansen using the (rescaled) mean-spherical approximation [72,73]. This potential is described at low ionic strength as:

$$u(r) = \begin{cases} \infty & r \le \sigma \\ \dfrac{z^2}{\pi\epsilon\epsilon_0(2+\kappa\sigma)^2} \cdot \dfrac{e^{-\kappa(r-\sigma)}}{r} & r > \sigma. \end{cases} \tag{2}$$

z is the charge of the macroions, ϵ_0 is the dielectric constant in vacuum and ϵ is the reduced dielectric constant of the solvent. σ is the diameter of the macroions and κ is the inverse Debye screening length [74],

$$\kappa = \sqrt{\frac{\sum_i n_i z_i^2}{\epsilon\epsilon_0 k_B T}}. \tag{3}$$

where n_i is concentration of ith component and k_B is Boltzmann constant. In addition to the long-ranged repulsion, when the effective attractions between proteins are not negligible, a two-Yukawa potential is very useful for describing these systems:

$$u(r) = \begin{cases} \infty & r \le \sigma \\ -K_1 \dfrac{e^{-Z_1(r-\sigma)}}{r} - K_2 \dfrac{e^{-Z_2(r-\sigma)}}{r} & r > \sigma. \end{cases} \tag{4}$$

Here, the first Yukawa term is used to describe the short-range attraction, Z_1 and K_1 correspond to the range and strength, respectively. The second term is used to describe the screened Coulomb repulsion. Thus, Z_2 and K_2 are related to the ionic strength and the net charge of the protein, respectively [43,75].

The model fits to the SAXS data are presented in Fig. 1. The model curves describes the scattering intensity as a function of q in the intermediate q range reasonably well. In the very low q region, the deviation from the experimental data is most likely due to the large clusters in the solution, whereas in the high q region, the scattering is mainly contributed from the individual proteins which are sensitive to the exact size and shape of the protein. While a simple ellipsoid as a form factor cannot fully capture the details of the protein, it does not significantly impact the data analysis on the protein interactions, namely the structure factor derived from data fitting. The corresponding structure factor and key parameters are presented in Fig. 3.

For BSA, Fig. 3a shows that S(q) in the low q region is below 0.2, while a strong correlation peak shifts towards higher q and increases in absolute value with increasing protein concentration. Increasing protein concentration from 20 mg/ml to 100 mg/ml, the fitted ionic strength (monovalent salt) in Fig. 3b increases first from about 3 mM to 30 mM, then reaches a plateau, which can be explained as the dissociation of ions from the residue groups on the protein surface and the dissociation rate decreases with increasing protein concentration. This value then decreases slightly above 200 mg/ml, suggesting that ion dissociation reaches equilibrium and that further increasing protein concentration reduces ion dissociation, which also explains the trends of surface charge in Fig. 3b. Using the experimentally determined volume fraction, the fitted surface charge decreases from 20 e to 12 e. Overall, the SC potential provides a reasonable description of the interactions, suggesting that long-range electrostatic repulsion induced by surface charge dominates the effective protein–protein interactions. It is worth noting that in our previous work [59], we employed the SC potential to fit SAXS data, with the volume fraction as a free parameter. The results indicated slightly larger fitted volume fractions compared to the experimentally determined values, but the resulting surface charge was around 10–15 e, lower than the present results.

For BLG, Fig. 3c reveals that S(q) from the two-Yukawa model increases in the low q region with increasing protein concentration, indicating enhanced attraction. In the meantime, a cluster–cluster correlation peak emerges above 13.2 mg/ml and shifts towards

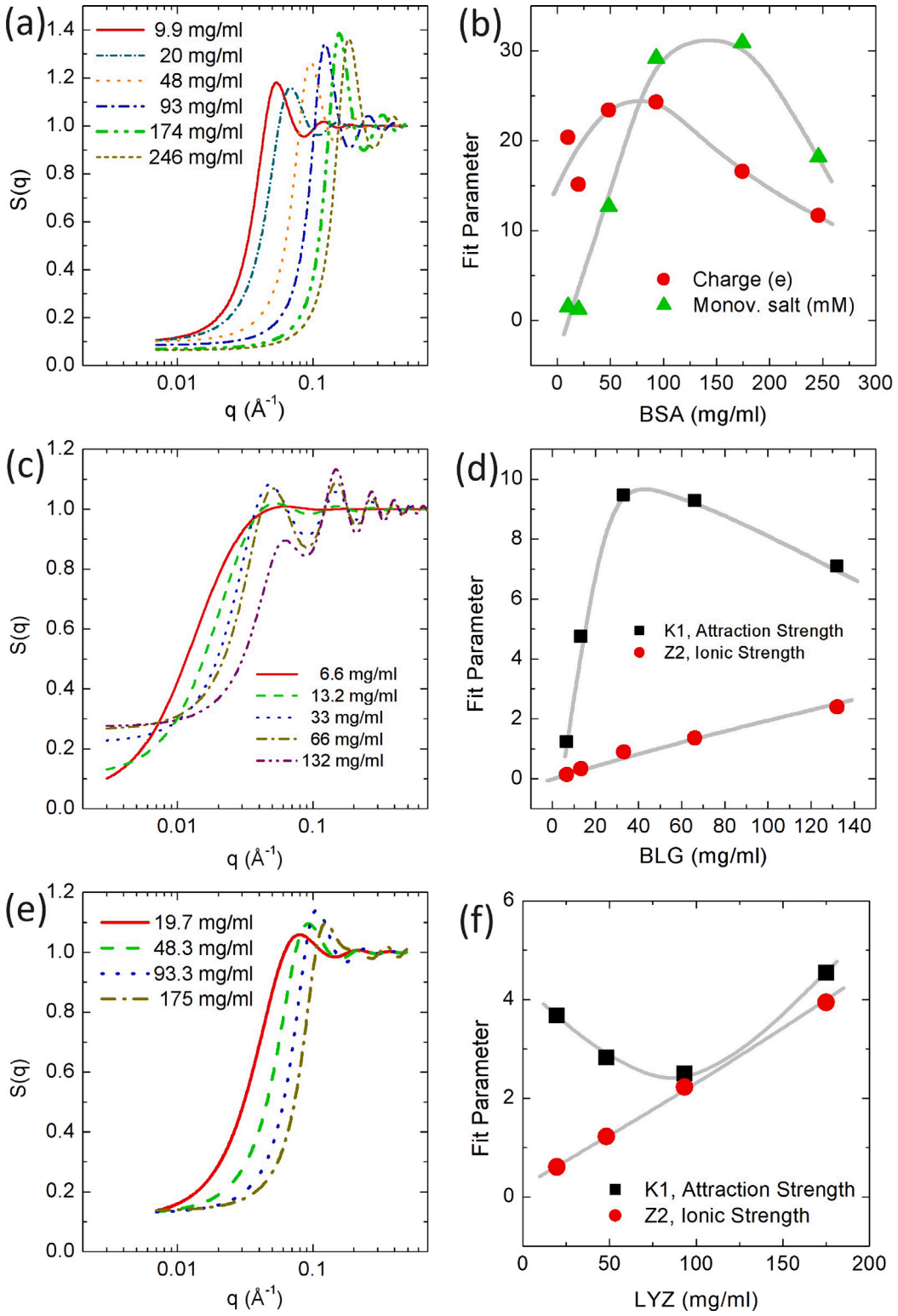

Fig. 3. Structure factor and the main control parameters from model fitting: (**a,b**) BSA. (**c,d**) BLG and (**e,f**) LYZ. The solid gray lines in (**b,d,f**) are the guide to the eye. Note the error bars for the fitting parameters from the fitting procedure are smaller than the symbol size, but we estimate the systematic error around 10%.

lower q values with increasing protein concentration, consistent with the reported results for LYZ under strong clustering conditions [43]. In the two-Yukawa model, the range of short-range attraction, Z_1 was fixed to 10, and the net charge of protein, K_2, was fixed to −2.5 for BLG and −5 for LYZ, respectively. The fitting parameter K_1 represents the strength of short-range attraction and Z_2 is related to the ionic strength of the solution. These parameters, determined from the fits, (Fig. 3d) are plotted as a function of protein concentration, indicating that increasing concentration initially leads to a stronger attraction (increases in K_1), followed by a slight decrease above 50 mg/ml due to the cluster formation at higher protein concentrations. The steady increase of Z_2 corresponds to an increase in ionic strength and a reduction of the Debye length.

For LYZ in Fig. 3e, S(q) profiles are similar to BSA with the peak position shifting towards higher q values. The fitting parameter of the two-Yukawa model (Fig. 3f) reveal a similar trend for Z_2 as observed for BLG, but K_1 shows an opposite trend, decreasing initially and then increasing. This trend can be explained by the pH change of the solution. The strength of attraction initially decreases due to the increase of surface charge, followed by an increase due to screening and stabilized surface charge (and pH).

3.2. Effect of ionic strength of added nacl on protein clustering and interactions

In this section, we investigate the effect of ionic strength on protein interactions and clustering behavior. For that we used the same three protein systems with a constant protein concentration while varying the concentration of added NaCl. SAXS results along with model fitting are presented in Fig. 4.

For BSA in Fig. 4a, the high q intensity remains unchanged as it is solely determined by the form factor. The lower q intensity increases with increasing ionic strength, leading to the broadening of the correlation peak. The resulting SC structure factor plots (Fig. 4d) exhibit a significant increase of S(q=0) and a slight shift of primary peak towards higher q. The results reveals that with increasing ionic strength enhances the surface net charge and slightly reduces the fitted volume fraction (Fig. 4d,g). Consequently, the strong reduction of the Debye length leads to the reduced the repulsion. This overall picture is consistent with the screening effect of added salt on charged proteins in solution [59].

For the BLG salt series in Fig. 4b, while the high q data remain unchanged with increasing ionic strength, the low q data show different behavior: without added salt, a pronounced correlation peak is visible. With increasing ionic strength, a similar trend to BSA is observed, i.e. the peak broadens and the low q intensity increases. However, above 100 mM, the intensity decreases, indicating the dissolution of protein clusters. The resulting two-Yukawa structure factor plots (Fig. 4e) reveal a cluster peak around $q = 0.05\,\text{Å}^{-1}$, which reduces its intensity with increasing ionic strength and eventually disappears above 100 mM. Model fitting results (Fig. 4h) demonstrate that increasing the ionic strength leads to a reduced strength of attraction (K_1), which explains the dissociation of the clusters (Fig. 4h).

In contrast to BSA and BLG, LYZ exhibits a distinct behavior with increasing ionic strength (Fig. 4c). Initially, for low ionic strength, increasing the salt concentration increases the scattering intensity in the low q region, similar to the other proteins, consistent with the overall screening effect of added salt on surface charges. However, upon further increasing the ionic strength above 100 mM, the low q intensity increases further, indicating an enhanced attraction. Model fitting using the two-Yukawa potential reveals that, contrary to BLG, increasing ionic strength in LYZ solutions leads to a stronger attraction, as evidenced by the increasing of K_1 (Fig. 4f,i). This enhanced attraction has been previously reported in LYZ solutions upon adding salts [7,38,70,71]. Tardieu and co-workers reported that a combination of a short-ranged attractive potential, such as the van der Waals potential, and a Coulombic repulsive correctly describe the phase behavior of LYZ solutions at different salt concentrations. Adding salt screens the electrostatic charges, reduces the repulsive strength, thus the effective interactions become more attractive. Furthermore, they found that at high ionic strength, the effective interactions show the ion specificities associated with the "Hofmeister series". [7]

3.3. Temperature dependence

Studies on lysozyme show a temperature dependent phase transition, and the interaction (attraction) is sensitive to temperature. The study by Stradner et al. [38] found that while the cluster peak positions are nearly constant in the concentration series, they shift to lower q and the total scattering intensity increases as the temperature decreases, meaning the effective attractions are enhanced. The consequence of the enhanced attraction is the formation of larger protein clusters. Increasing salt concentration screens the electrostatic charges, also favoring larger clusters. Similar temperature enhanced attraction in LYZ solutions has been reported by other studies. [41,70]

Both LYZ and BLG solutions with and without salt at two temperatures (10 and 25 °C) were studied by SAXS. BSA solutions are not sensitive in this temperature range. [76] Fig. 5(a) shows the results of BLG solutions and it is clear to see that the SAXS profiles for two temperatures nearly overlap, indicating that changing temperature from 10 to 25 °C does not change the effective interactions. In contrast, SAXS profiles for LYZ show a salt concentration dependence in Fig. 5(b). Without added salt or with only 20 mM NaCl, the SAXS profiles have the same shape, but careful comparison indicates the intensity at the peak position (and the low q-region) increases when the temperature decreases from 25 to 10 °C, indicating the enhanced attraction. This enhancement becomes even stronger for LYZ solutions with higher salt concentration. With 100 and 200 mM NaCl, the Screened Coulombic potential is strongly reduced, and the scattering intensity at $q = 0.1\,\text{Å}^{-1}$ are significantly enhanced. While lysozyme solutions show exactly the same behavior as reported in literature,[38,40,41] i.e. enhanced attraction on decreasing the temperature, no visible change could be seen for BLG solutions at the same temperatures. Thus a model fit was not performed for these SAXS data.

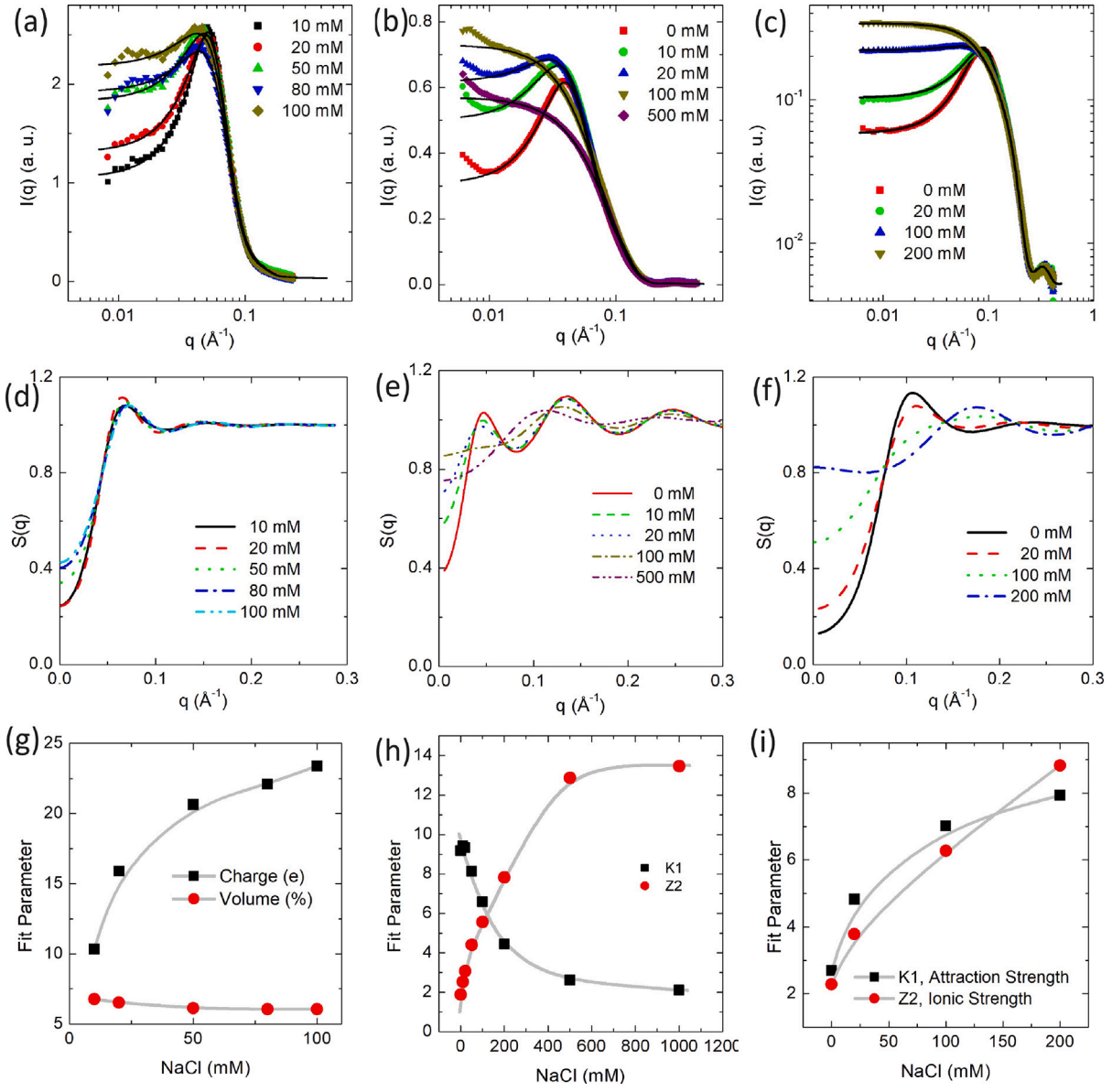

Fig. 4. Effects of ionic strength on the effective interactions: SAXS profiles (a) 93 mg/ml BSA (b) 66 mg/ml BLG (c) Lysozyme 93 mg/ml. The solid black lines are the corresponding data fits. Corresponding structure factors S(q) in (d), (e), (f) and the fitting parameters in (g), (h), (i). Note the error bars for the fitting parameters from the fitting procedure are smaller than the symbol size, but we estimate the systematic error around 10%.

4. Discussion and conclusions

We now summarize and compare the three protein systems. For non-clustering BSA in solution, the effective interactions are dominated by the surface charge, which overwhelms the possible attraction, such as van der Waals interaction. This is well-captured by the screened Coulomb structure factor, which accurately describes the SAXS data. Increasing ionic strength by adding NaCl reduces the Debye length, diminishing the strength and range of electrostatic interactions. Additionally, the absence of clustering ensures that the average inter-protein distance conforms to the 1/3 power law. All three proteins are globular proteins and carry net charges in neutral solutions. BSA and BLG have pI values below 7, resulting in net negative charges, while LYZ has a pI of 10.8, bearing positive charges. These surface charges engender a long-range electrostatic repulsion between proteins, evident in the strong correlation peaks observed in SAXS profiles.

Protein clustering is often attributed to the delicate balance between long-range electrostatic repulsion and an additional short-range attraction. While the long-range repulsion is predominantly driven by protein surface charges in all three systems, the nature of the short-range attraction may vary significantly. Our study reveals distinct responses of these three systems to changes in

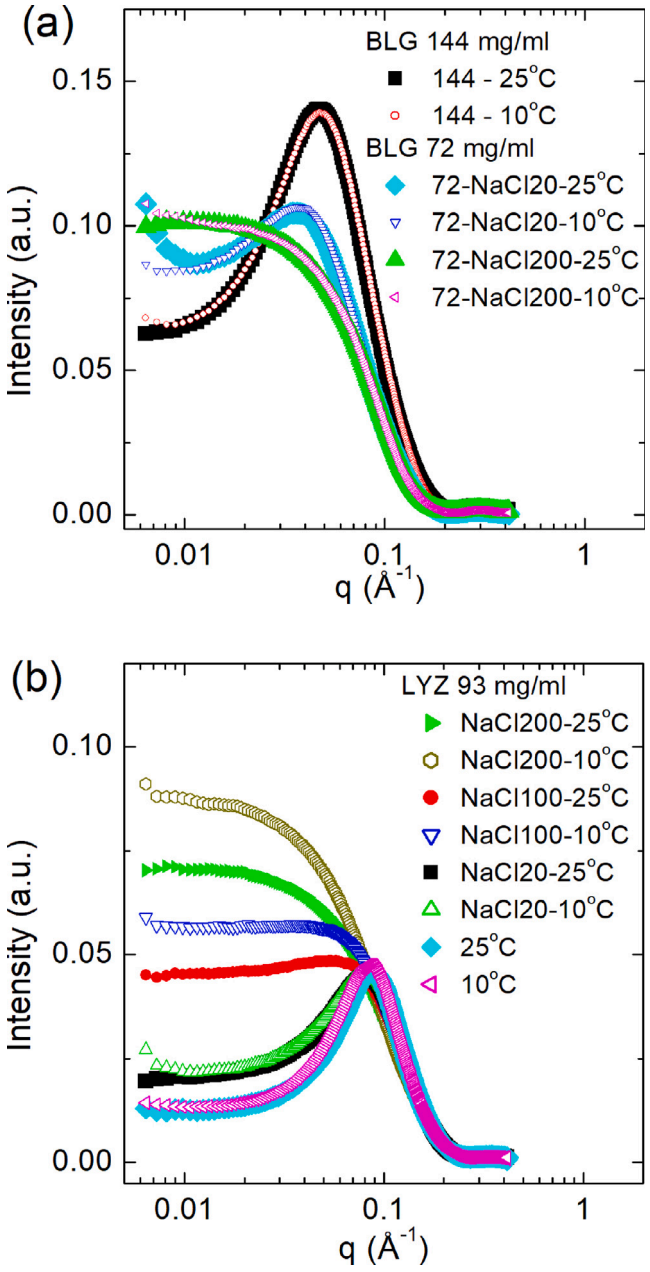

Fig. 5. Temperature dependent SAXS profiles at 25 and 10 °C for (**a**) BLG 144 mg/ml, 72 mg/ml with 20 and 200 mM NaCl, and (**b**) LYZ 93 mg/mL with 0, 20 and 200 mM NaCl.

ionic strength and temperature, particularly for BLG and LYZ. These differences suggest diverse underlying attraction mechanisms. Quantitative fitting of SAXS data reveals that the attraction for LYZ is enhanced with increasing ionic strength or decreasing temperature, indicating the non-Coulombic nature of the attraction. Literature suggests that this attraction arises predominantly from van der Waals interactions. [7,70,71]

For BLG, the attraction reduces with increasing ionic strength but exhibits insensitivity to temperature fluctuations, suggesting that the attractions between proteins are more specific, possibly arising from complementary charge patterns on the protein surface. These specific interactions can be reduced by ion screening but remain unaffected by temperature changes. A systematic study by Piazza and co-workers on one of the two variants of BLG, i.e. BLGA, has provided valuable insights into protein interactions and cluster formation [77,78]. Their findings revealed that BLGA molecules in solution exhibit strong attractions, leading to the formation of transient clusters. However, this clustering effect can be fully suppressed by adding electrolytes, which is in good agreement with our observation that BLG clustering is reduced by increasing ionic strength (Fig. 4). Additionally, they found that the absolute

values of the surface charges of BLGA molecules are similar but have opposite signs under the experimental conditions employed. This observation implies that the effective interactions between proteins depend on the specific distribution of surface charges.

The results of this study provide compelling evidence that protein clustering is highly sensitive to the nature of the short-range attraction, suggesting that it can be manipulated to fine-tune the clustering properties of proteins. The strikingly contrasting behaviors of these proteins in solution also emphasize the need for a deeper understanding of interactions of charged macromolecules, which are crucial for predicting protein clustering and phase behavior.

CRediT authorship contribution statement

Fajun Zhang: Writing – review & editing, Writing – original draft, Validation, Supervision, Resources, Project administration, Methodology, Investigation, Funding acquisition, Formal analysis, Data curation, Conceptualization. **Michal K. Feustel:** Writing – review & editing, Writing – original draft, Validation, Methodology, Investigation, Formal analysis, Data curation, Conceptualization. **Maximilian W.A. Skoda:** Writing – review & editing, Validation, Formal analysis, Data curation. **Robert M.J. Jacobs:** Writing – review & editing, Validation, Formal analysis, Data curation. **Felix Roosen-Runge:** Writing – review & editing, Validation, Formal analysis, Data curation, Conceptualization. **Tilo Seydel:** Writing – review & editing, Validation, Formal analysis, Data curation, Conceptualization. **Michael Sztucki:** Validation, Methodology, Data curation. **Frank Schreiber:** Writing – review & editing, Writing – original draft, Supervision, Project administration, Funding acquisition, Conceptualization.

Declaration of competing interest

The authors declare that they have no known competing financial interests or personal relationships that could have appeared to influence the work reported in this paper.

Data availability

Data will be made available on request.

Acknowledgments

We acknowledge financial support from the Deutsche Forschungsgemeinschaft (DFG), Germany and BMBF (05K20VTA). We thank T. Stehle and C. Schall (Tübingen) for sharing lab resources, and assistance during characterization experiments. Furthermore we thank the ESRF for allocation of beamtime.

References

[1] V.J. Anderson, H.N.W. Lekkerkerker, Insights into phase transition kinetics from colloid science, Nature 416 (6883) (2002) 811–815, URL http://www.nature.com/nature/journal/v416/n6883/abs/416811a.html.
[2] S.D. Durbin, G. Feher, Protein crystallization, Annu. Rev. Phys. Chem. 47 (1) (1996) 171–204, http://dx.doi.org/10.1146/annurev.physchem.47.1.171.
[3] P.G. Vekilov, Dense liquid precursor for the nucleation of ordered solid phases from solution, Cryst. Growth Des. 4 (4) (2004) 671–685, http://dx.doi.org/10.1021/cg049977w, URL http://pubs.acs.org/doi/abs/10.1021/cg049977w.
[4] R.P. Sear, Interactions in protein solutions, Curr. Opin. Colloid Interface Sci. 11 (1) (2006) 35–39, http://dx.doi.org/10.1016/j.cocis.2005.09.003, URL http://www.sciencedirect.com/science/article/pii/S1359029405000610.
[5] M. Muschol, F. Rosenberger, Liquid–liquid phase separation in supersaturated lysozyme solutions and associated precipitate formation/crystallization, J. Chem. Phys. 107 (6) (1997) 1953–1962, http://dx.doi.org/10.1063/1.474547, URL http://link.aip.org/link/?JCP/107/1953/1.
[6] R. Piazza, Protein interactions and association: An open challenge for colloid science, Curr. Opin. Colloid Interface Sci. 8 (6) (2004) 515–522, http://dx.doi.org/10.1016/j.cocis.2004.01.008, URL http://www.sciencedirect.com/science/article/B6VRY-4C12CT3-3/2/e727ccf8c7e68124a2a39c080b6be2f0.
[7] A. Tardieu, A. Le Verge, M. Malfois, F. Bonneté, S. Finet, M. Riès-Kautt, L. Belloni, Proteins in solution: from X-ray scattering intensities to interaction potentials, J. Cryst. Growth 196 (2–4) (1999) 193–203, http://dx.doi.org/10.1016/S0022-0248(98)00828-8, URL http://www.sciencedirect.com/science/article/pii/S0022024898008288.
[8] R. Piazza, Interactions and phase transitions in protein solutions, Curr. Opin. Colloid Interface Sci. 5 (1–2) (2000) 38–43, http://dx.doi.org/10.1016/S1359-0294(00)00034-0, URL http://www.sciencedirect.com/science/article/B6VRY-414WV0R-6/2/3ce7c0cc536285846017befc4ef2488c.
[9] A. Stradner, H. Sedgwick, F. Cardinaux, W.C.K. Poon, S.U. Egelhaaf, P. Schurtenberger, Equilibrium cluster formation in concentrated protein solutions and colloids, Nature 432 (2004) 492–495.
[10] J. Gunton, A. Shiryayev, D. Pagan, Protein Condensation: Kinetic Pathways to Crystallization and Disease, Cambridge University Press, 2007.
[11] C.P. Brangwynne, C.R. Eckmann, D.S. Courson, A. Rybarska, C. Hoege, J. Gharakhani, F. Jülicher, A.A. Hyman, Germline P granules are liquid droplets that localize by controlled dissolution/condensation, Science 324 (5935) (2009) 1729–1732, 10.1126/science.1172046.
[12] L.L. Goff, T. Lecuit, Phase transition in a cell, Science 324 (5935) (2009) 1654–1655, 10.1126/science.1176523.
[13] Y. Li, V. Lubchenko, M.A. Vorontsova, L. Filobelo, P.G. Vekilov, Ostwald-like ripening of the anomalous mesoscopic clusters in protein solutions, J. Phys. Chem. B 116 (35) (2012) 10657–10664, http://dx.doi.org/10.1021/jp303316s, URL http://www.ncbi.nlm.nih.gov/pubmed/22889282.
[14] L.-P. Bergeron-Sandoval, N. Safaee, S.W. Michnick, Mechanisms and consequences of macromolecular phase separation, Cell 165 (5) (2016) 1067–1079.
[15] J.J. McManus, P. Charbonneau, E. Zaccarelli, N. Asherie, The physics of protein self-assembly, Curr. Opin. Colloid Interface Sci. 22 (2016) 73–79.
[16] D. Fusco, P. Charbonneau, Soft matter perspective on protein crystal assembly, Colloids Surf. B 137 (2016) 22–31.
[17] R.A. Curtis, H.W. Blanch, J.M. Prausnitz, Calculation of phase diagrams for aqueous protein solutions, J. Phys. Chem. B 105 (12) (2001) 2445–2452, http://dx.doi.org/10.1021/jp003087j, URL http://pubs.acs.org/doi/abs/10.1021/jp003087j.
[18] R.A. Curtis, J.M. Prausnitz, H.W. Blanch, Protein–protein and protein–salt interactions in aqueous protein solutions containing concentrated electrolytes, Biotechnol. Bioeng. 57 (1) (1998) 11–21, http://dx.doi.org/10.1002/(SICI)1097-0290(19980105)57:1<11::AID-BIT2>3.0.CO;2-Y.

[19] K.D. Collins, Ions from the Hofmeister series and osmolytes: Effects on proteins in solution and in the crystallization process, Methods 34 (3) (2004) 300–311, http://dx.doi.org/10.1016/j.ymeth.2004.03.021, URL http://www.sciencedirect.com/science/article/pii/S1046202304001124.
[20] D. Rosenbaum, P. Zamora, C. Zukoski, Phase behavior of small attractive colloidal particles, Phys. Rev. Lett. 76 (1) (1996) 150–153, URL http://link.aps.org/doi/10.1103/PhysRevLett.76.150.
[21] M. Muschol, F. Rosenberger, Interactions in undersaturated and supersaturated lysozyme solutions: Static and dynamic light scattering results, J. Chem. Phys. 103 (1995) 10424, http://dx.doi.org/10.1063/1.469891.
[22] O.D. Velev, E.W. Kaler, A.M. Lenhoff, Protein interactions in solution characterized by light and neutron scattering: Comparison of lysozyme and chymotrypsinogen, Biophys. J. 75 (6) (1998) 2682–2697, http://dx.doi.org/10.1016/S0006-3495(98)77713-6.
[23] J.A. Thomson, P. Schurtenberger, G.M. Thurston, G.B. Benedek, Binary liquid phase separation and critical phenomena in a protein/water solution, Proc. Natl. Acad. Sci. USA 84 (20) (1987) 7079–7083, http://www.pubmedcentral.nih.gov/articlerender.fcgi?artid=299233&tool=pmcentrez&rendertype=abstract.
[24] Y. Liu, E. Fratini, P. Baglioni, W.-R. Chen, S.-H. Chen, Effective long-range attraction between protein molecules in solutions studied by small angle neutron scattering, Phys. Rev. Lett. 95 (2005) 118102, http://dx.doi.org/10.1103/PhysRevLett.95.118102, URL http://link.aps.org/doi/10.1103/PhysRevLett.95.118102.
[25] F. Zhang, Nonclassical nucleation pathways in protein crystallization, J. Phys.: Condens. Matter. 29 (44) (2017) 443002.
[26] F. Zhang, F. Roosen-Runge, A. Sauter, M. Wolf, R.M.J. Jacobs, F. Schreiber, Reentrant condensation, liquid-liquid phase separation and crystallization in protein solutions induced by multivalent metal ions, Pure Appl. Chem. 86 (2014) 191–202.
[27] F. Zhang, M.W.A. Skoda, R.M.J. Jacobs, S. Zorn, R.A. Martin, C.M. Martin, G.F. Clark, S. Weggler, A. Hildebrandt, O. Kohlbacher, F. Schreiber, Reentrant condensation of proteins in solution induced by multivalent counterions, Phys. Rev. Lett. 101 (14) (2008) 148101, http://dx.doi.org/10.1103/PhysRevLett.101.148101, URL http://link.aps.org/abstract/PRL/v101/e148101.
[28] F. Zhang, S. Weggler, M.J. Ziller, L. Ianeselli, B.S. Heck, A. Hildebrandt, O. Kohlbacher, M.W.A. Skoda, R.M.J. Jacobs, F. Schreiber, Universality of protein reentrant condensation in solution induced by multivalent metal ions, Proteins 78 (16) (2010) 3450–3457.
[29] P. Lindner, T. Zemb, Neutrons, X-rays, and Light: Scattering Methods Applied to Soft Condensed Matter, Elsevier North-Holland, 2002.
[30] D. Bendedouch, S.-H. Chen, Structure and interparticle interactions of bovine serum albumin in solution studied by small-angle neutron scattering, J. Chem. Phys. 87 (9) (1983) 1473–1477, URL http://pubs.acs.org/doi/abs/10.1021/j100232a003.
[31] R. Nossal, C.J. Glinka, S.-H. Chen, SANS studies of concentrated protein solutions. I. Bovine serum albumin, Biopolymers 25 (6) (1986) 1157–1175, http://dx.doi.org/10.1002/bip.360250613.
[32] N. Ise, T. Okubo, S. Kunugi, H. Matsuoka, K. Yamamoto, Y. Ishii, "Ordered" structure in dilute solutions of sodium polystyrenesulfonates as studied by small-angle X-ray scattering, J. Chem. Phys. 81 (7) (1984) 3294–3306.
[33] N. Begam, S. Da Vela, O. Matsarskaia, M.K. Braun, A. Mariani, F. Zhang, F. Schreiber, Packing and dynamics of a protein solution approaching the jammed state, Soft Matter 16 (33) (2020) 7751–7759.
[34] W. Häußler, A. Wilk, J. Gapinski, A. Patkowski, Interparticle correlations due to electrostatic interactions: A small angle X-ray and dynamic light scattering study. I. Apoferritin, J. Chem. Phys. 117 (2002) 413.
[35] W. Häußler, Neutron spin echo studies on ferritin: free-particle diffusion and interacting solutions, Eur. Biophys. J. 37 (2008) 563–571.
[36] L. Ianeselli, F. Zhang, M.W.A. Skoda, R.M.J. Jacobs, R.A. Martin, S. Callow, S. Prévost, F. Schreiber, Protein-protein interactions in ovalbumin solutions studied by small-angle scattering: Effect of ionic strength and the chemical nature of cations, J. Phys. Chem. B 114 (11) (2010) 3776–3783.
[37] P. Baglioni, E. Fratini, B. Lonetti, S.H. Chen, Structural arrest in concentrated cytochrome C solutions: The effect of pH and salts, J. Phys.: Condens. Matter. 16 (42) (2004) S5003, URL http://stacks.iop.org/0953-8984/16/i=42/a=016.
[38] A. Stradner, F. Cardinaux, P. Schurtenberger, A small-angle scattering study on equilibrium clusters in lysozyme solutions, J. Phys. Chem. B 110 (42) (2006) 21222–21231, http://dx.doi.org/10.1021/jp0639804, URL http://www.ncbi.nlm.nih.gov/pubmed/17048949.
[39] F. Cardinaux, A. Stradner, P. Schurtenberger, F. Sciortino, E. Zaccarelli, Modeling equilibrium clusters in lysozyme solutions, Europhys. Lett. 77 (2007) 48004, http://dx.doi.org/10.1209/0295-5075/77/48004, URL http://iopscience.iop.org/0295-5075/77/4/48004.
[40] F. Cardinaux, E. Zaccarelli, A. Stradner, S. Bucciarelli, B. Farago, S.U. Egelhaaf, F. Sciortino, P. Schurtenberger, Cluster-driven dynamical arrest in concentrated lysozyme solutions, J. Phys. Chem. B 115 (22) (2011) 7227–7237, http://dx.doi.org/10.1021/jp112180p, URL http://pubs.acs.org/doi/abs/10.1021/jp112180p.
[41] A. Shukla, E. Mylonas, E. Di Cola, S. Finet, P. Timmins, T. Narayanan, D.I. Svergun, Absence of equilibrium cluster phase in concentrated lysozyme solutions, Proc. Natl. Acad. Sci. USA 105 (13) (2008) 5075–5080, http://dx.doi.org/10.1073/pnas.0711928105, URL http://www.pnas.org/content/105/13/5075.abstract.
[42] L. Porcar, P. Falus, W.-R. Chen, A. Faraone, E. Fratini, K. Hong, P. Baglioni, Y. Liu, Formation of the dynamic clusters in concentrated lysozyme protein solutions, J. Phys. Chem. Lett. 1 (1) (2010) 126–129, http://dx.doi.org/10.1021/jz900127c, URL http://pubs.acs.org/doi/abs/10.1021/jz900127c.
[43] Y. Liu, L. Porcar, J. Chen, W.-R. Chen, P. Falus, A. Faraone, E. Fratini, K. Hong, P. Baglioni, Lysozyme protein solution with an intermediate range order structure, J. Phys. Chem. B 115 (22) (2011) 7238–7247, http://dx.doi.org/10.1021/jp109333c, URL http://pubs.acs.org/doi/abs/10.1021/jp109333c.
[44] M.K. Braun, M. Grimaldo, F. Roosen-Runge, I. Hoffmann, O. Czakkel, M. Sztucki, F. Zhang, F. Schreiber, T. Seydel, Crowding-controlled cluster size in concentrated aqueous protein solutions: Structure, self- and collective diffusion, J. Phys. Chem. Lett. 8 (2017) 2590–2596, http://dx.doi.org/10.1021/acs.jpclett.7b00658.
[45] P.D. Godfrin, N.E. Valadez-Pérez, R. Castañeda-Priego, N.J. Wagner, Y. Liu, Generalized phase behavior of cluster formation in colloidal dispersions with competing interactions, Soft Matter 10 (2014) 5061.
[46] S. Das, J. Riest, R.G. Winkler, G. Gompper, J.K.G. Dhont, G. Nagele, Clustering and dynamics of particles in dispersions with competing interactions: Theory and simulation, Soft Matter 14 (1) (2018) 92–103.
[47] D. Stopper, R. Roth, Phase behavior and bulk structural properties of a microphase former with anisotropic competing interactions: A density functional theory study, Phys. Rev. E 96 (4) (2017) 042607, PRE.
[48] J.A. Bollinger, T.M. Truskett, Fluids with competing interactions. I. Decoding the structure factor to detect and characterize self-limited clustering, J. Chem. Phys. 145 (2016) 064902.
[49] J.A. Bollinger, T.M. Truskett, Fluids with competing interactions. II. Validating a free energy model for equilibrium cluster size, J. Chem. Phys. 145 (2016) 064903.
[50] E. Mani, W. Lechner, W.K. Kegel, P.G. Bolhuis, Equilibrium and non-equilibrium cluster phases in colloids with competing interactions, Soft Matter 10 (25) (2014) 4479–4486.
[51] P.D. Godfrin, R. Castañeda-Priego, Y. Liu, N.J. Wagner, Intermediate range order and structure in colloidal dispersions with competing interactions, J. Chem. Phys. 139 (2013) 154904.
[52] C. Beck, M. Grimaldo, F. Roosen-Runge, R. Maier, O. Matsarskaia, M. Braun, B. Sohmen, O. Czakkel, R. Schweins, F. Zhang, T. Seydel, F. Schreiber, Following protein dynamics in real time during crystallization, Crystal Growth Des. 19 (12) (2019) 7036–7045.
[53] M. Grimaldo, F. Roosen-Runge, F. Zhang, F. Schreiber, T. Seydel, Dynamics of proteins in solution, Q. Rev. Biophys. 52 (2019) e7.
[54] General discussion, Faraday Discuss. 159 (2012) 139–180.

[55] S. Barhoum, A. Yethiraj, NMR detection of an equilibrium phase consisting of monomers and clusters in concentrated lysozyme solutions, J. Phys. Chem. B 114 (2010) 17062–17067, http://dx.doi.org/10.1021/jp108995k, URL http://pubs.acs.org/doi/abs/10.1021/jp108995k.
[56] H.A. Sober, CRC Handbook of Biochemistry: Selected Data for Molecular Biology, The Chemical Rubber Co. Cleveland, Ohio, 1970.
[57] R. Borsali, R. Pecora (Eds.), Synchroton small-angle X-ray scattering, in: Soft Matter Characterization, Springer, New York, 2008.
[58] T. Narayanan, M. Sztucki, P.V. Vaerenbergh, J. Leonardon, J. Gorini, L. Claustre, F. Sever, J. Morse, P. Boesecke, A multipurpose instrument for time-resolved ultra-small-angle and coherent X-ray scattering, Journal of Applied Crystallography 51 (6) (2018) 1511–1524, https://doi.org/10.1107/S1600576718012748, in press, URL http://www.sciencedirect.com/science/article/pii/0006300263905997.
[59] F. Zhang, M.W.A. Skoda, R.M.J. Jacobs, R.A. Martin, C.M. Martin, F. Schreiber, Protein interactions studied by SAXS: Effect of ionic strength and protein concentration for BSA in aqueous solutions, J. Phys. Chem. B 111 (1) (2007) 251–259, http://dx.doi.org/10.1021/jp0649955, URL http://pubs.acs.org/doi/abs/10.1021/jp0649955.
[60] O. Glatter, O. Kratky, Small Angle X-Ray Scattering, Academic Press London, United States Edition New York, 1982.
[61] D.I. Svergun, M.H.J. Koch, Small-angle scattering studies of biological macromolecules in solution, Rep. Progr. Phys. 66 (10) (2003) 1735–1782, URL http://stacks.iop.org/0034-4885/66/i=10/a=R05.
[62] J.-P. Hansen, I.R. McDonald, Theory of Simple Liquids, third ed., Academic Press Amsterdam, 2006.
[63] S.-H. Chen, Small angle neutron scattering studies of the structure and interaction in micellar and microemulsion systems, Annu. Rev. Phys. Chem. 37 (1) (1986) 351–399.
[64] A. Isihara, Determination of molecular shape by osmotic measurement, J. Chem. Phys. 18 (11) (1950) 1446–1449, http://dx.doi.org/10.1063/1.1747510, URL http://link.aip.org/link/?JCP/18/1446/1.
[65] F. Zhang, F. Roosen-Runge, M.W.A. Skoda, R.M.J. Jacobs, M. Wolf, P. Callow, H. Frielinghaus, V. Pipich, S. Prevost, F. Schreiber, Hydration and interactions in protein solutions containing concentrated electrolytes studied by small-angle scattering, Phys. Chem. Chem. Phys. 14 (2012) 2483–2493, http://dx.doi.org/10.1039/C2CP23460B.
[66] S.R. Kline, Reduction and analysis of SANS and USANS data using IGOR Pro, J. Appl. Crystallogr. 39 (6) (2006) 895–900, http://dx.doi.org/10.1107/S0021889806035059.
[67] L.R. Barbosa, M.G. Ortore, F. Spinozzi, P. Mariani, S. Bernstorff, R. Itri, The importance of protein-protein interactions on the pH-induced conformational changes of bovine serum albumin: A small-angle X-Ray scattering study, Biophys. J. 98 (1) (2010) 147–157, http://dx.doi.org/10.1016/j.bpj.2009.09.056, URL http://www.sciencedirect.com/science/article/pii/S0006349509015707.
[68] M. Verheul, J.S. Pedersen, S.P.F.M. Roefs, K.G. de Kruif, Association behavior of native β-lactoglobulin, Biopolymers 49 (1) (1999) 11–20, http://dx.doi.org/10.1002/(SICI)1097-0282(199901)49:1<11::AID-BIP2>3.0.CO;2-1.
[69] U.M. Elofsson, M.A. Paulsson, T. Arnebrant, Adsorption of β-lactoglobulin A and B in relation to self-association:?effect of concentration and pH, Langmuir 13 (6) (1997) 1695–1700, http://dx.doi.org/10.1021/la9601061, URL http://pubs.acs.org/doi/abs/10.1021/la9601061.
[70] M. Malfois, F. Bonneté, L. Belloni, A. Tardieu, A model of attractive interactions to account for fluid-fluid phase separation of protein solutions, J. Chem. Phys. 105 (1996) 3290–3300.
[71] F. Bonneté, S. Finet, A. Tardieu, Second virial coefficient: Variations with lysozyme crystallization conditions, J. Cryst. Growth 196 (2–4) (1999) 403–414, http://dx.doi.org/10.1016/S0022-0248(98)00826-4, URL http://www.sciencedirect.com/science/article/pii/S0022024898008264.
[72] J.B. Hayter, J. Penfold, An analytic structure factor for macroion solutions, Mol. Phys. 42 (1) (1981) 109–118, URL http://www.informaworld.com/10.1080/00268978100100091.
[73] J.-P. Hansen, J.B. Hayter, A rescaled MSA structure factor for dilute charged colloidal dispersions, Mol. Phys. 46 (3) (1982) 651–656, URL http://www.informaworld.com/10.1080/00268978200101471.
[74] J. Israelachvili, Intermolecular and Surface Forces, Academic Press, London, 1991.
[75] Y. Liu, W.-R. Chen, S.-H. Chen, Cluster formation in two-Yukawa fluids, J. Chem. Phys. 122 (4) (2005) 044507, http://dx.doi.org/10.1063/1.1830433, URL http://link.aip.org/link/?JCP/122/044507/1.
[76] O. Matsarskaia, L. Bühl, C. Beck, M. Grimaldo, R. Schweins, F. Zhang, T. Seydel, F. Schreiber, F. Roosen-Runge, Evolution of the structure and dynamics of bovine serum albumin induced by thermal denaturation, Phys. Chem. Chem. Phys. 22 (33) (2020) 18507–18517.
[77] R. Piazza, S. Iacopini, Transient clustering in a protein solution, Eur. Phys. J. E 7 (1) (2002) 45–48, http://dx.doi.org/10.1140/epje/i200101179.
[78] R. Piazza, S. Iacopini, M. Galliano, BLGA protein solutions at high ionic strength: Vanishing attractive interactions and “frustrated” aggregation, Europhys. Lett. 59 (2002) 149–154.